OPEN

Gene Therapy (2017), 1–9

www.nature.com/gt

SHORT COMMUNICATION

MR-guided parenchymal delivery of adeno-associated viral vector serotype 5 in non-human primate brain

L Samaranch[1,3], B Blits[2,3], W San Sebastian[1], P Hadaczek[1], J Bringas[1], V Sudhakar[1], M Macayan[1], PJ Pivirotto[1], H Petry[2] and KS Bankiewicz[1]

The present study was designed to characterize transduction of non-human primate brain and spinal cord with AAV5 viral vector after parenchymal delivery. AAV5-CAG-GFP (1×10^{13} vector genomes per milliliter (vg ml^{-1})) was bilaterally infused either into putamen, thalamus or with the combination left putamen and right thalamus. Robust expression of GFP was seen throughout infusion sites and also in other distal nuclei. Interestingly, thalamic infusion of AAV5 resulted in the transduction of the entire corticospinal axis, indicating transport of AAV5 over long distances. Regardless of site of injection, AAV5 transduced both neurons and astrocytes equally. Our data demonstrate that AAV5 is a very powerful vector for the central nervous system and has potential for treatment of a wide range of neurological pathologies with cortical, subcortical and/or spinal cord affection.

Gene Therapy advance online publication, 16 March 2017; doi:10.1038/gt.2017.14

INTRODUCTION

Neurological gene therapy development with adeno-associated virus-based vectors (AAV), besides improvements in production methods leading to higher titers of vector, has been marked by three seminal discoveries. First, pressurized parenchymal infusions of different AAV serotypes by convection-enhanced delivery (CED) yield much more widespread distribution in the brain than simple injection does.[1] Sequential innovations have steadily improved CED, particularly with the advent of reflux-resistant cannulae and MR-guided visualization of infusions.[2–5] Second, AAV serotypes exhibit distinct cellular specificities with some neuronally restricted, such as AAV2 or AAV6, and others with preference for either neurons or astrocytes, such as AAV7 or AAV9.[6–10] This cellular specificity has important immunological implications for expression of non-self proteins over prolonged periods of time.[11,12] Finally, AAV serotypes are transported along axons and thereby direct expression in anatomical regions distal to the primary vector infusion site. This latter discovery has obvious implications to the clinical development of therapies for neurological disorders. Anatomical connectivity facilitates the spread of viral particles and enhances brain distribution of the therapeutic gene. Interestingly, it has been found that the directionality of the transport is serotype dependent.[6] The most representative and well-characterized serotype is AAV serotype 2. Direct infusion of AAV2 into the thalamus resulted in an anterograde transport of vector particles to cortical layers IV and V over a wide territory from prefrontal to occipital cortex[13] and from putamen to substantia nigra pars reticulata (SNpr) in rats and non-human primate (NHP).[14,15] Recently, however, we studied in NHP the axonal transport of AAV2 prepared by methods that differed sharply from the standard preparation technique.[16,17] To our surprise, this formulation was axonally transported in a retrograde direction and was not completely neuron-specific.[18] We surmise that anterograde axonal transport of AAV2 may be not be an intrinsic property of AAV2 itself but perhaps may be directed by the presence of strongly bound adventitious proteins that seem to be present in standard preparations and can be removed by stringent washing.[19] In contrast, the neurotropic AAV6 is axonally transported exclusively in a retrograde direction.[6,20] Infusion of AAV6 into putamen yielded abundant transgene expression in cortical and thalamic projecting neurons to striatum suggesting that nerve terminals took up viral particles and transported to the neuronal cell bodies harbored in distal anatomically connected structures. Recently, axonal transport of AAV serotype 9 has also been characterized.[21–23] Putaminal infusions revealed transport to thalamus and cortex as well as substantia nigra pars compacta. This pattern indicates that AAV9 underwent retrograde transport, however, SNpr, a region that receives projections from putamen, also showed transgene expression indicating anterograde transport of AAV9 as well. Further analysis demonstrated that the bidirectional transport of serotype 9 is dose dependent.[21] Dose range study with different viral loads showed a dose requirement for effective transport, more pronounced on anterograde-linked structures to the injection site than on distal structures that synapse with the target structure.[21] Although the field is growing in knowledge on the specifics of different serotypes, there is still a need to identify and characterize more new serotypes with different and more robust performance to expand the current choices of viral vectors with great potential for clinical indication. In addition, the ability to generate recombinant AAV using a reliable and scalable baculovector-mediated technology will certainly aid vector development and boost its application in the gene therapy field.

In that regards, the AAV serotype 5 has shown great potential for different indications in small animal models and dogs[24–26] but

[1]Department of Neurological Surgery, University of California, San Francisco, CA, USA and [2]Neurobiology, Research and Development, UniQure NV, Amsterdam 1105BA, The Netherlands. Correspondence: Professor KS Bankiewicz, Department of Neurological Surgery, University of California, 1855 Folsom Street, MCB 226, San Francisco, CA 94103-0555, USA.
E-mail: Krystof.Bankiewicz@ucsf.edu
[3]These authors contributed equally to this work.
Received 9 September 2016; revised 19 January 2017; accepted 1 February 2017

the characterization of axonal transport in large animals is still missing. Deep understanding of AAV5 vector performance regarding transport and distribution will allow a more precise therapeutic indication. For this reason in the present study we characterized axonal transport of the AAV serotype 5 after parenchymal delivery in primates. The study results suggest that AAV5 has significant potential for indications where more global transduction of the brain and spinal cord is required.

RESULTS AND DISCUSSION

Anterograde transport of AAV5-GFP viral particles

All putaminal infusions were performed with MR-guided CED. Each hemisphere received 51 µl of AAV5 encoding green fluorescent protein gene (GFP) at 1.0×10^{13} vg ml^{-1} (5.1×10^{11} vg per hemisphere). Histological analysis of the brain showed identically robust localized distribution of GFP within both putamina and transduction that extended slightly laterally through the claustrum (arrowheads, Figure 1a). Direct protein sequence and biochemistry comparison determined that AAV5 serotype is markedly different than AAV2 in terms of capsid conformation.[27] These differences among serotypes may affect viral particle dissemination due to variable features such as capsid stability, receptor binding, intercellular trafficking and intracellular genome release.[28] In that sense, three-dimensional (3D) reconstruction of the infusate gadolinium signal in the MRI (Figure 1b) revealed that after delivering 51 µl per side (volume of infusion; Vi), the volume of distribution (Vd) was ~3 times larger (Vd^{left}: 155 µl; Vd^{right}: 150 µl). This coefficient was higher compared with AAV2 that has a Vd/Vi ratio of about 2.[5]

Histological analysis revealed that putaminal medium spiny neurons were highly transduced in the area of injection along the primary area of distribution (Figure 1c). Based on cellular morphology, immunohistochemical analysis of representative sections indicated the presence of transduced neurons and astrocytes at the infusion site. No signal was found in caudate nucleus, thalamus (Figure 1d) or cortex (Figure 1e). Only distal structures innervated by the putamen showed extensive GFP expression (Figure 1f). In particular, SNpr, a structure that receives projections from the striatum through striato-nigral projections, showed high levels of GFP expression in the terminals (Figure 1g). Similarly, globus pallidus also contained GFP-positive fibers (Figure 1h). These results suggest robust anterograde transport of the AAV5 viral particles through striatal projections, either directly by striato-nigral or indirectly by striato-pallidal pathways. In addition, the lack of any signal in the cortex would indicate the absence of retrograde transport via cortico-striatal projections. No GFP was found in cervical, thoracic or lumbar levels of the spinal cord (Figure 1i). Based on these findings, AAV5 most closely resembles AAV serotype 2 with respect to axonal transport and cell transduction, albeit more efficient.

Dose-dependent retrograde transport of AAV5-GFP viral particles

A second animal received bilateral infusions into thalamus also by MR-guided CED. Each hemisphere received a larger volume of vector (199 µl; 2×10^{13} vg per hemisphere) than received by the animal with injection only into putamen (51 µl; 5.1×10^{12} vg per hemisphere). Both thalamic infusions resulted in robust localized distribution of GFP-immunoreactive (GFP-ir) cells, both neurons and glia, within both targets (Figure 2a). Moreover, transduction extended laterally into the external capsule and posterior

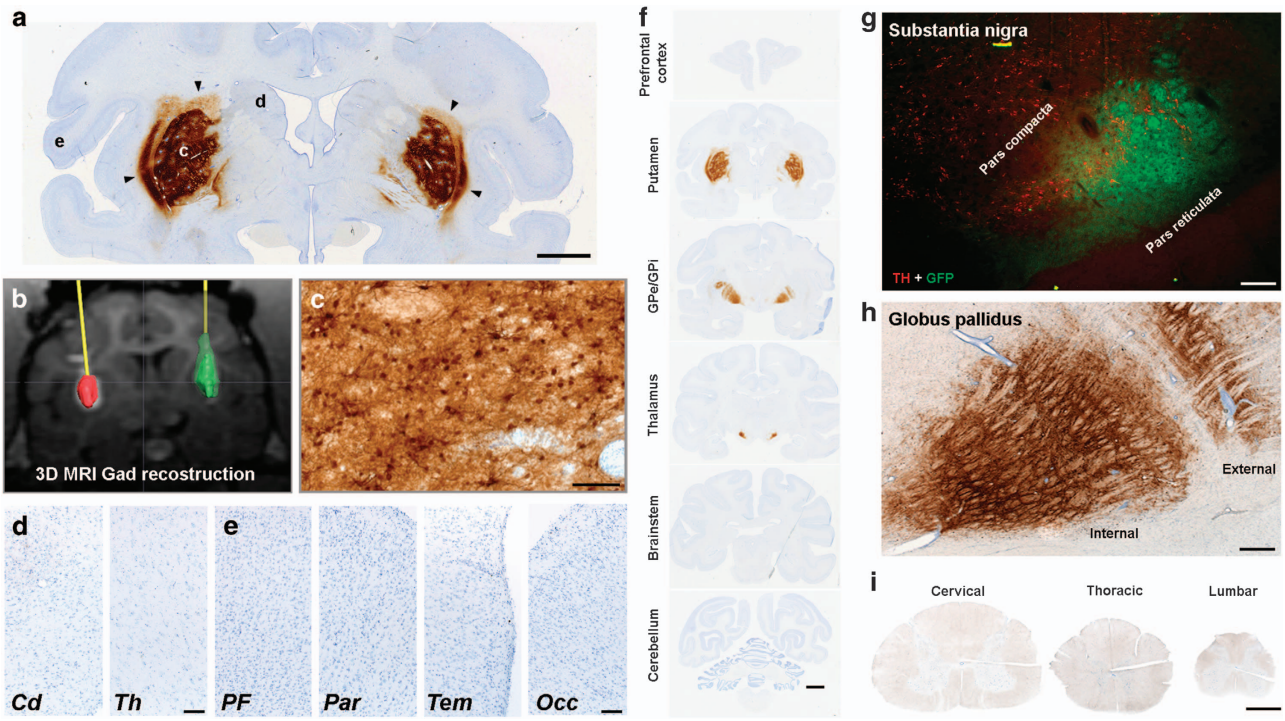

Figure 1. GFP expression after bilateral delivery of AAV5-CAG-GFP into putamen. GFP immunostaining (brown) showed optimal coverage at the injection sites of both putamina (**a**). Gadolinium signal was mostly contained within target structures as shown in the 3D MRI reconstruction (**b**). Strong signal was found in the injection site (**c**), while no GFP signal was detected in other subcortical regions like caudate or thalamus (**d**). No cortical transport was found as revealed by the absence of GFP-transduced cells in different parts of the cortex (**e**) and other subcortical areas (**f**). Only substantia nigra pars reticulata (**g**) and globi pallidi (**h**) were found transduced. No transduced motor neurons were found in the spinal cord along cervical, thoracic or lumbar regions (**i**). Sections were processed with DAB immunostaining counterstained with Nissl (blue). Scale bars = 5 mm for **a** and **f**; 100 µm for **c**–**e**; 500 µm for **g** and **h**; 2 mm for **i**. Cd, caudate nucleus; GP, globus pallidus; Occ, occipital cortex; Par, parietal cortex; PF, pre-frontal cortex; Tem, temporal cortex; Th, thalamus; TH, tyrosine hydroxylase.

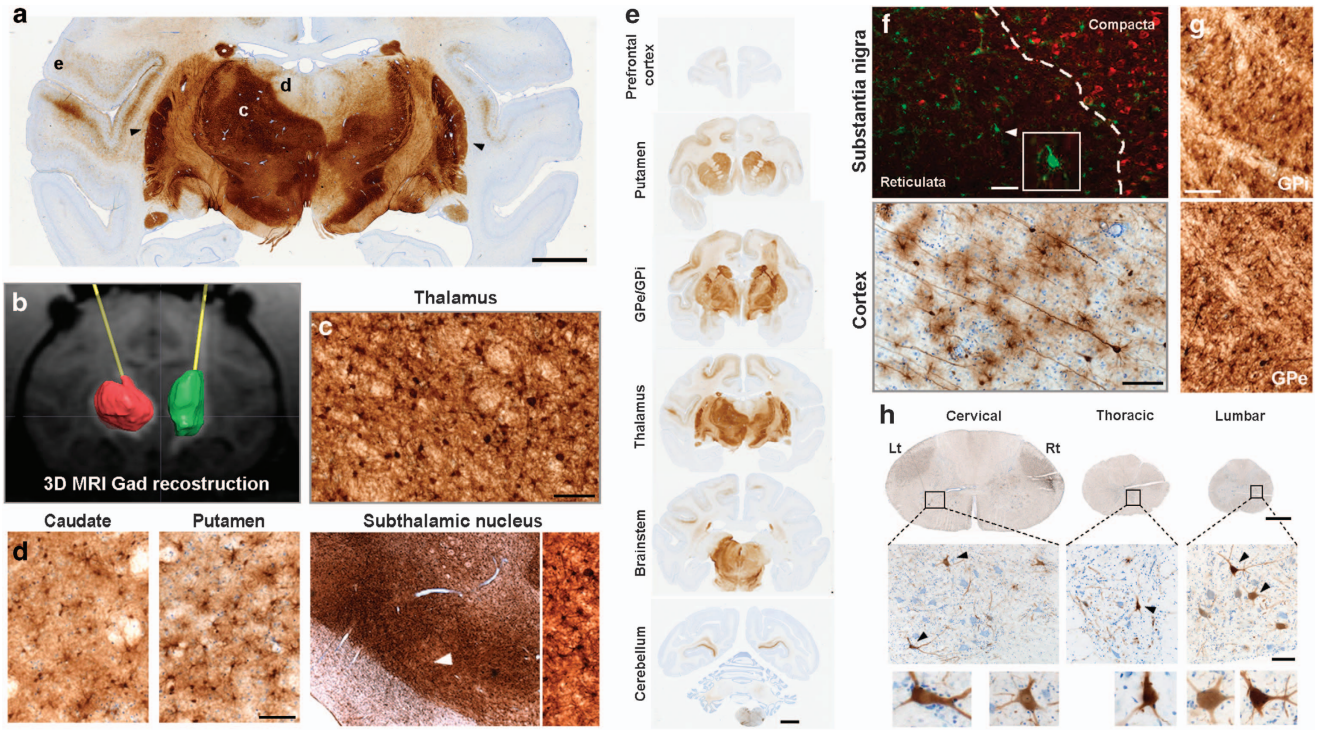

Figure 2. GFP expression after bilateral delivery of AAV5-CAG-GFP into thalamus. DAB immunostaining (brown) illustrating GFP expression derived from bilateral vector delivery into the thalamus (**a**). Gadolinium signal was mostly contained within target structures as shown in the 3D MRI reconstruction (**b**). Strong cellular transduction occurred primarily at the brain nuclei receiving the AAV5 vector infusion (**c**). In contrast to putaminal infusion, GFP-positive cells were detected in distal brain regions such as caudate, putamen and subthalamic nucleus (**d**). Cortical transduction was also found along antero-posterior axis of the brain (**e**). Interestingly, positive GFP cells were found in substantia nigra reticulata (**f**) and globi pallidi (**g**), suggesting retrograde transport after thalamic infusion. Strong motor neuron transduction was found in the spinal cord along cervical, thoracic or lumbar regions (**h**). Sections were processed with DAB immunostaining counterstained with Nissl (blue). Scale bars = 5 mm for **a** and **e**; 100 μm for **c**, **f** (bottom), **g** and **h** (bottom); 200 μm for **d** and **f** (top); 2 mm for **h** (top). Insets are digital magnification to show details of the areas pointed by white or black arrowheads.

putamen (arrowheads, Figure 2a). During parenchymal infusion, reflux occurred up the outside of the cannula in the right hemisphere (Supplementary Figure 1a), which decreased the internal pressure of the bolus and reduced Vi (<199 μl). Consequently, only the left hemisphere showed a Vd ~3 times larger than the Vi (Vd^{left}: 561 μl/Vi^{left}: 199 μl) in the 3D analysis of the gadolinium signal from the thalamic infusate (Figure 2b). The right hemisphere showed a Vd/Vi coefficient of ~2 (456 μl/199 μl), suggesting that pressurized delivery ensures the efficient dispersion of the viral particles throughout the target structure. More importantly, the suboptimal delivery also affected the axonal transport. The backflow occurrence (Supplementary Figure 1b) became an excellent opportunity to evaluate back-to-back axonal transport after different doses. Macroscopically, differences in the levels of expression between hemispheres were found, mostly in pre-frontal and frontal cortices, whereas the levels of expression in the injection sites were the same. This result suggests a link between dose (total viral particles infused) and the directionality of the axonal transport.

Microscopic analysis showed that thalamic neurons were highly transduced along the injection site and primary area of distribution after infusion (Figure 2c), as well as in caudate, putamen and subthalamic nucleus (Figure 2d). All these structures receive projections from the thalamus, suggesting anterograde transport of viral particles. Interestingly, this animal also showed high GFP expression levels in distal structures (Figure 2e) thus SNpr, cortex (Figure 2f) and globus pallidus (Figure 2g), structures that project neurons to the thalamus. GFP-ir neurons in these structures would indicate retrograde transport as well. This retrograde transport was not seen in the animal that received putaminal injection alone, which had no GFP signal in the cortex. Emborg and colleagues recently described how vector titer could affect vector distribution. In their experience, identical volumes with different vector concentration revealed a positive direct correlation between high titers and large distribution pattern of protein expression.[29] In the present study, thalamic infusion delivered a total dose of viral capsids 3.9-fold higher that in the putaminal infusion alone (2.0×10^{12} vg vs 0.51×10^{12} vg, respectively). Our results show that titer not only activates transport but also regulates direction, suggesting a dose-dependent retrograde transport.

A third animal received a combined putaminal and thalamic MR-guided infusion of AAV5-GFP. The left hemisphere received 125 μl of AAV5-GFP at 1.0×10^{13} vg ml^{-1} (1.3×10^{12} total vg) into the putamen, and right hemisphere received 200 μl of AAV5-GFP at 1×10^{13} vg ml^{-1} ($2.\times10^{12}$ total vg) into the thalamus. Compared with the other two groups in this experiment, this animal received the same amount of total viral capsids into the thalamus, but 2.5-fold higher in the putamen.

Analysis of GFP staining showed widespread cortical and subcortical expression of GFP transgene throughout the anterior–posterior axis in both brain hemispheres, regardless of the location of the infusion (Figure 3a). 3D analysis of the MRI contrast revealed that the Vd of the putamen and the thalamus was also threefold larger than Vi (Figures 3b and c), consistent with previous infusions. No reflux occurred along the needle track during delivery.

GFP covered the thalamus in the right hemisphere (Figure 3b) and GFP-ir cells were found in homolateral putamen and subthalamic nucleus, structures that receive projections from

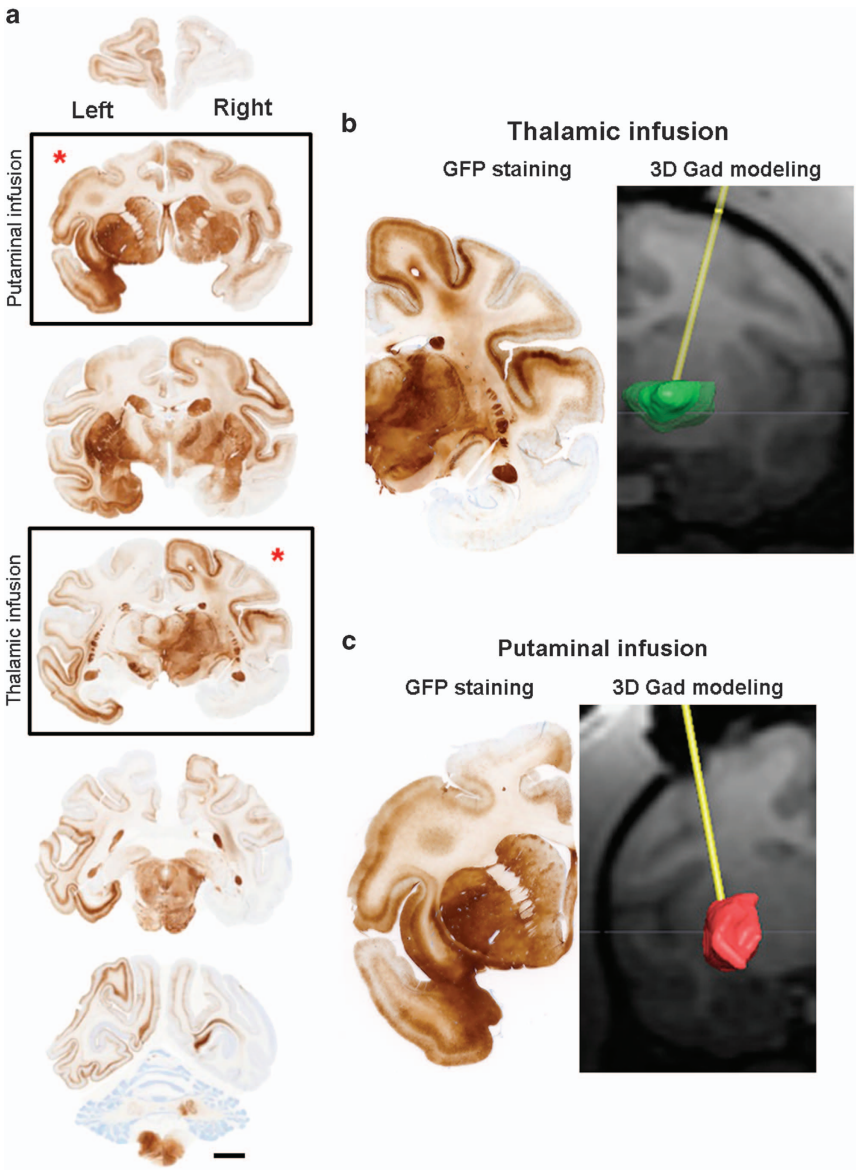

Figure 3. GFP expression after delivery of AAV5-CAG-GFP into left putamen and right thalamus. Infusion of AAV5-CAG-GFP vector into the brain resulted in a widespread expression of the transgene throughout target structures for all animals. DAB immunostaining (brown) showed GFP expression into cortical and subcortical structures along prefrontal and occipital regions of the brain. Histology analysis of the anatomical targets showed a massive transduction both after thalamic (**b**) and putaminal infusions (**c**). Sections were processed with DAB immunostaining counterstained with Nissl (blue). Scale bars = 5 mm for **a**.

thalamus (Figure 4a), supporting our finding that AAV5 undergoes anterograde transport. Nevertheless, GFP-positive cells were also found in SNpr and GPi (Figure 4a), indicating that AAV5 is also retrogradely transported. Cerebral cortex, from frontal to occipital region, was highly transduced through cortico-thalamo-cortical loop (Figure 4a). This topological distribution of GFP-ir cell was identical to what was observed after the bilateral thalamic infusion.

On the other hand, histologic analysis of the putaminal injection in the left hemisphere revealed considerable differences from the previous putaminal infusion. High levels of GFP transduction were present at the injection site (Figure 3c). Distal structures were also analyzed and GFP signal was found in the terminals of the striato-nigral projections, confirming the presence of anterograde transport. But, unlike what was observed after the bilateral putaminal infusion, GFP-positive neurons were found in cerebral cortex, thalamus and substantia nigra pars compacta, regions that project to the putamen, confirming that AAV5 viral particles underwent retrograde transport (Figure 4b), even after putaminal injection. Similarly to the bilateral thalamic infusion, the combined number of particles for putaminal delivery was also higher than the previous one (2.5-fold higher). In our hands, high doses of AAV5 in the range of $1.0–1.5 \times 10^{12}$ total vg, triggers retrograde transport of the vector, if properly delivered into the brain, clearly suggesting that retrograde axonal transport is dose dependent.

Spinal transduction after intracerebral infusion of AAV5-GFP viral particles

As in the putaminal infusion, spinal cord was also analyzed in the animals that received AAV5 vector in the thalamus. Besides the ascending and descending fibers that form the thalamo-cortico-thalamic and the striato-cortical projections, thalamus and cortex also connect with spinal cord. Ventral posterior-lateral nucleus of the thalamus synapses with ascending axons that arise mainly

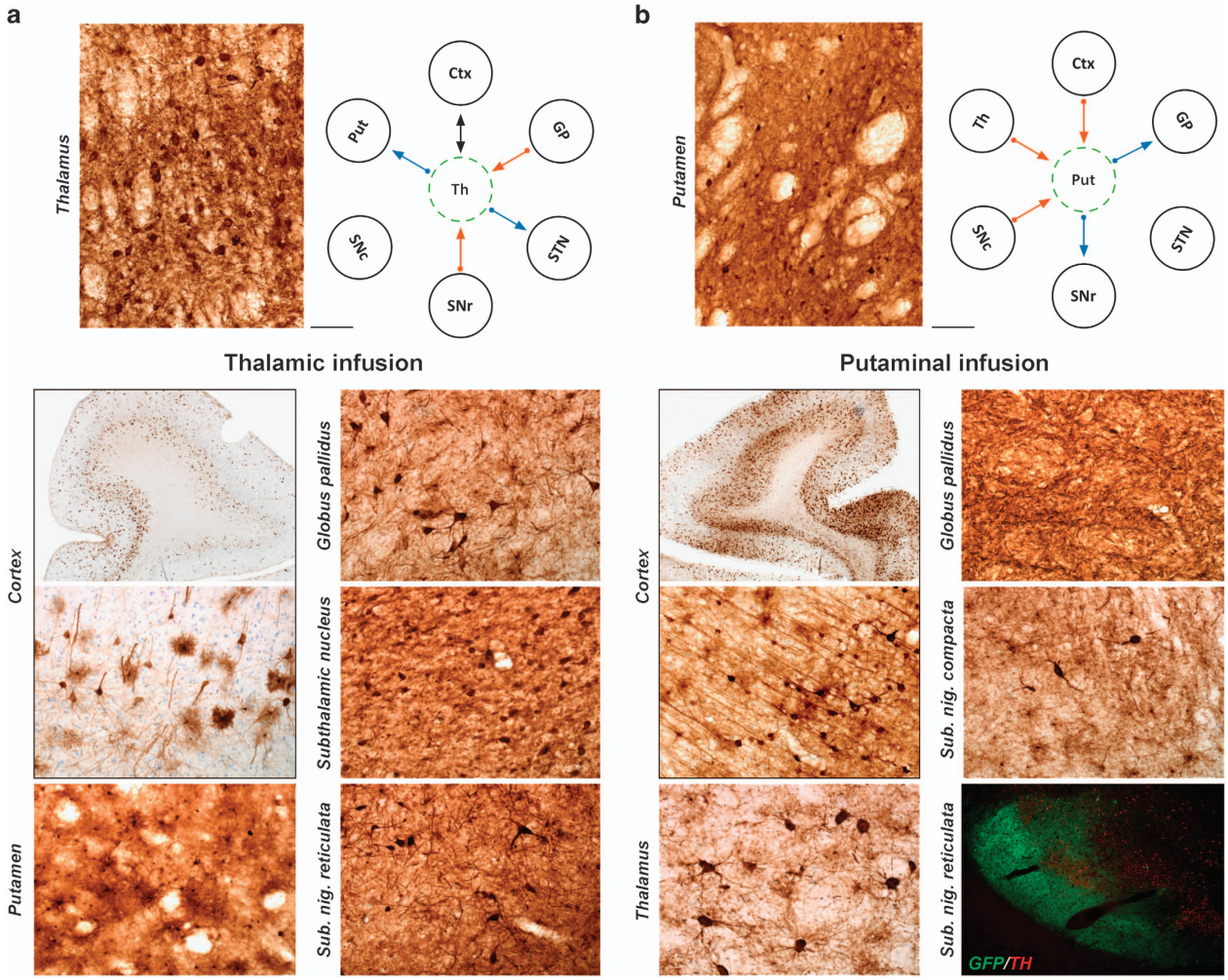

Figure 4. Axonal transport after thalamic and putaminal combined delivery of AAV5-CAG-GFP. Delivery of AAV5-GFP vector in a combined approach resulted in a more extensive vector propagation along cortical and subcortical brain structures. Thalamic injection on the left hemisphere (**a**) showed GFP-positive cells in structures that receive thalamic projections like putamen and subthalamic nucleus (anterograde transport, blue arrows), and in brain nuclei that project to thalamus like globus pallidus and substantia nigra pars reticulate (retrograde transport, orange arrows). Putaminal injection on the right hemisphere (**b**) showed GFP-positive cells in structures that project to putamen like thalamus and SNpc (retrograde transport, orange arrows), while structures that receive putaminal projections like globus pallidus and substantia nigra pars reticulata showed GFP-positive fibers (anterograde transport, blue arrows). Scale bars = 100 μm for **a** and **b**. Ctx, cortex; GP, globus pallidus; Put, putamen; SNpc, substantia nigra pars compacta; STN, subthalamic nucleus; Th, thalamus; TH, tyrosine hydroxylase.

from the dorsal horn of the lumbar region through the spino-thalamic pathway, but the motor cortex projects long axons that synapse with spinal motor neurons through cortico-spinal tract. Interestingly, histological analysis of the spinal cord after parenchymal injection revealed high GFP transduction of motor neurons of the ventral horn at all spinal levels in both animals (Figures 2h and 5a). This signal is most likely due to anterograde transport of AAV5 from transduced cortical neurons through the cortico-spinal tracts, whereas the GFP found in the contra-lateral dorsal horns (Figure 5b) and dorsal root ganglia entry zone (Figure 5c) is probably due to retrograde transport of the viral particles through the spino-thalamic projections. Sections from different levels along these two tracts were also analyzed and GFP expression was found in all main structures, such as pyramidal cells in cortical layer V, posterior limb of the internal capsule, pontine nucleus, brainstem and medulla (Supplementary Figure 2).

The remarkable degree of transduction of corticospinal tracts by AAV5 is unprecedented in our experience and suggests that this serotype may be of great utility in the treatment of central nervous system diseases, such as amyotrophic lateral sclerosis (ALS) and multiple sclerosis, in which the pathology is evident in cortical, brainstem and spinal tissues.

Immunological consequences of AAV5-mediated GFP expression

Neutralizing antibodies (nAb) titers against AAV5 and GFP were measured in serum samples collected prior to surgery (baseline) and at necropsy (8 weeks after vector delivery). All the animals were found to be seronegative before brain delivery with anti-AAV5 nAb titers of $\leqslant$ 1:100. Animals received different total doses of viral particles distributed in different total volumes (Table 1). Eight weeks after surgery, analysis of sera samples showed that anti-AAV5 and anti-GFP antibody titers increased drastically in all cases. The animal with bilateral infusion into the putamen received the lowest vector dose and molecular analysis revealed an anti-capsid increase of 851-fold at necropsy. On the other hand, the animal that received the combination (three times more viral particles) generated 908-fold more anti-AAV5 antibodies at the end of the study. The last animal (bilateral thalamus) received the largest total viral load and the serum levels correlated with the highest production of nAb, a 1488-fold increase. Although these

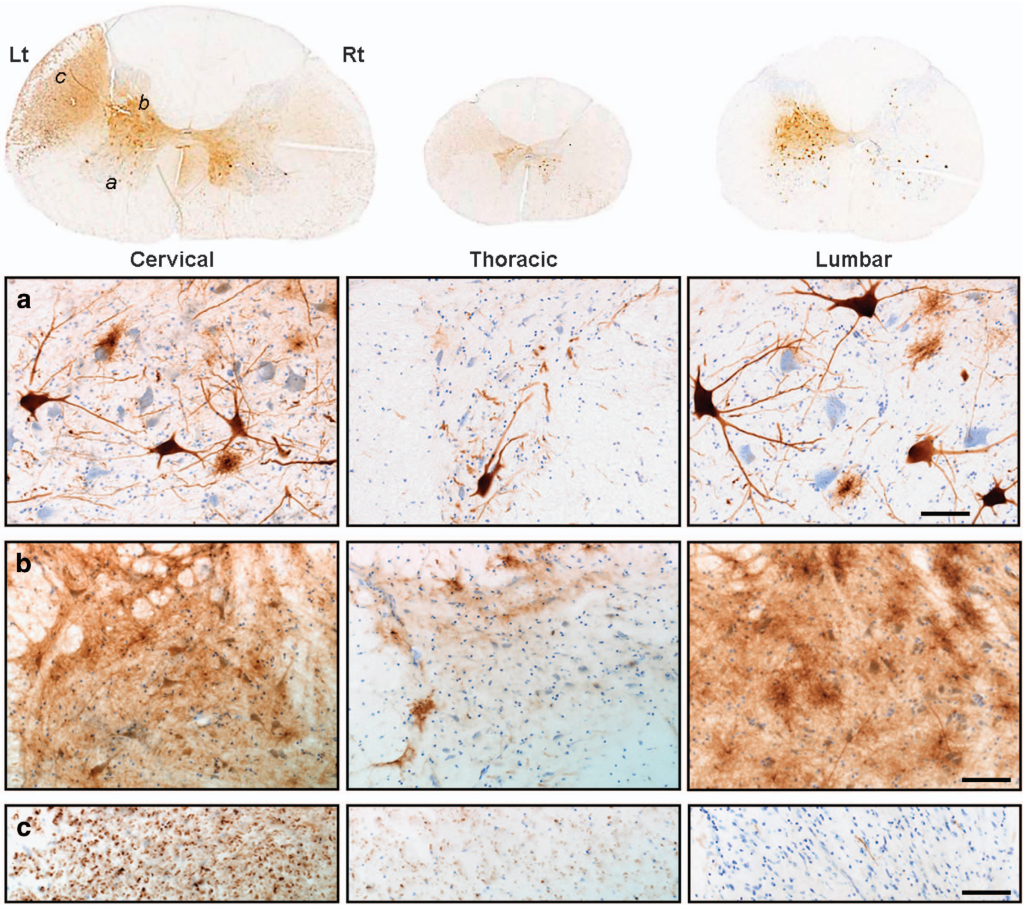

Figure 5. Expression of GFP in spinal cord after thalamic/putaminal infusion of AAV5-CAG-GFP. GFP-positive motor neurons were present in the ventral horns at all levels of the spinal cord (**a**). GFP signal was found also in dorsal horns at all levels (**b**) and at the dorsal root ganglia entrance (**c**), being more pronounced at cervical than in the other levels. Scale bars = 100 μm for **a**–**c**.

Table 1. Treatment group assignments

Group/Route	*Survival (weeks)*	*Concentration (vg ml^{-1})*	*Volume (μl)*		*Total dose (vg × 10^{12})*		
			Left	*Right*	*Left*	*Right*	*Total*
Parenchymal delivery							
Putamen bilateral ($n = 1$)	8	1.0×10^{13}	51	51	0.51	0.51	1.02
Left putamen/right thalamus ($n = 1$)	8	1.0×10^{13}	125	200	1.3	2.0	3.3
Thalamus bilateral ($n = 1$)	8	1.0×10^{13}	200	200	2.0	2.0	4.0

data showed a positive correlation with the vector dose, the magnitude of the anti-AAV5 nAb production was the same (Supplementary Figure 3a). A similar trend was found when anti-GFP nAb were analyzed, showing similar immune response regardless of the final vector genome titer infused (Supplementary Figure 3b).

Cellular tropism was also analyzed by immunostaining. Results revealed that AAV5 serotype, as previously described[30] and other serotypes such as AAV9 or AAV7,[10] is capable of transducing both neurons and astrocytes (Supplementary Figure 3c), and indicates that AAV5 also has potential for therapies that would require vast transduction of glial cells, for example, *GDNF* or *NRF2* therapies against amyotrophic lateral sclerosis.[31–33] However, when the vector carries a foreign protein, an immunological response is expected.[11,12] Tissue analysis of the injection sites revealed that AAV5 vector carrying a non-self recognized protein triggered a full immune reaction after being infused into the cerebral parenchyma. H&E staining revealed significant cellular infiltration near the vessels both in putamen and thalamus (Supplementary Figure 4a). Moreover, astrocytes and microglia were strongly activated (Supplementary Figures 4b and c) while MHC-II was upregulated as well (Supplementary Figure 4d). All these markers indicated a clear ongoing immune reaction. NeuN staining was also performed in all animals and some staining lacunae were found surrounding the needle tracts at the infusion sites, indicating some neuronal toxicity in areas with high levels of GFP expression. Nevertheless, none of the animals presented any clinical signs throughout the study.

This immunotoxicity is a phenomenon seen with other serotypes, notably AAV9, driving expression of non-self proteins. As we have pointed out previously,[34] such antigen presentation only may be a significant concern with prolonged expression of

foreign, or non-self-recognized transgenes. In clinical studies, in which self-proteins are being expressed, this type of immunotoxicity should not be a problem, no matter whether the serotype is showing astrocytic tropism or not.

In summary, this exploratory study suggests that AAV5 has considerable potential for the delivery of therapeutic candidate genes, where more global transduction of the brain is required, such as neurological pathologies ranging from Huntington disease to lysosomal storage disorders or spinal disorders. Even so, further experiments are necessary to obtain a more comprehensive description of the dose-dependent axonal transport.

MATERIALS AND METHODS

Animals

Three male adult Cynomolgus macaques (*Macaca fascicularis*; 6.45–6.61 kg) were included in this exploratory study (Table 1). Animals were screened for the presence of anti-AAV antibodies prior to dosing and at termination as previously described.[35] All animals were considered seronegative with neutralizing antibody titers lower than 1:100 at baseline.

In-life observations

Since AAV5 encoded the gene for GFP, a foreign protein, an immune reaction was expected as previously described.[12] Therefore, veterinary personnel monitored all animals after AAV delivery until the end of the study to identify any possible adverse effects. Cage-side observations were performed twice daily throughout the study to evaluate general health, appearance, and appetite in all animals. Animals were weighed prior to surgery, weekly for the first 4 weeks after surgery, and biweekly thereafter until the conclusion of the study. None of the animals showed any adverse effects.

Vector design and production

The AAV5 vector encoding the cDNA of the enhanced GFP gene was packaged into AAV5 by a baculovirus-based method at Amsterdam Molecular Therapeutics (uniQure NV) as previously described,[36,37] resulting in a single-stranded rAAV vector. Briefly, the GFP coding sequence was preceded at the 5′ end by a Kozak sequence and at the 3′ end by the bovine growth hormone polyadenylation signal. The complete transcription unit was flanked by two non-coding AAV-derived inverted terminal repeats, and expression was driven by a CAG promoter, a combination of the cytomegalovirus early enhancer element and chicken β-actin promoter. For vector production, Sf9 insect cells were infected by three recombinant baculoviruses; (i) encoding *rep* for replication and packaging, (ii) *cap*-5 for the AAV5 capsid and (iii) with the expression cassette. *Cap*-5 sequence was adapted and optimized to the baculovirus-mediated assembly of rAAV. Although *Cap*-5 sequence maintained its original amino acid sequence, the optimization process (patent pending) improved its assembly ability and increase infectivity of the resulting AAV vector (patent pending). After viral particle assembled, prep purification was performed with AVB Sepharose high-performance affinity medium (GE Healthcare, Piscataway, NJ, USA). Vector concentration was determined by quantitative PCR with primer-probe combinations directed against the transgene and the one with highest packaging rate was selected for study. The final titer of the vector preparation was 1.4×10^{14} vg ml^{-1}.

The single vector dilution assigned to parenchymal infusion (1.0×10^{13} vg ml^{-1}) was spiked with gadolinium chelate (2 mM, Prohance, Bracco Diagnostics, Princeton, NJ, USA) to visualize delivery during the MR-guided infusion.[4] All drugs were prepared on the day of surgery by dilution of vector with phosphate-buffered saline (PBS) and 5% sucrose.

MR-guided vector delivery

Animals were randomly assigned for the parenchymal infusions of virus into putamen ($n = 1$), thalamus ($n = 1$) or both ($n = 1$). Volumes and titers of different injections are described in Table 1.

Brain delivery. Briefly, animals were sedated (intramuscular ketamine (10 mg kg^{-1}) and medetomidine (0.015 mg kg^{-1})), intubated and maintained under anesthesia with isoflurane (1–3% v/v). Then, animals were placed supine in an MR-compatible stereotactic frame and, after craniotomy, underwent stereotactic placement of MR-compatible, skull-mounted, temporary ball-joint cannula guides over each hemisphere.[38] Animals were then moved into the MRI (GE 1.5T MRI mobile unit, DMS, Imaging Reno, NV, USA) to determine the trajectory to target brain nuclei inside the brain. Once the trajectory was determined, a ceramic custom-designed fused silica reflux-resistant cannula with a 3-mm stepped tip was used for the infusion.[1,4,39,40] Infusion rate was ramped up to a maximum of 3 µl min^{-1}. Once the infusion ended, skull-mounted guide devices were removed and animals were taken back to their home cages and monitored during recovery from anesthesia.

Tissue collection and section processing

Animals were transcardially perfused first with PBS and then with 4% paraformaldehyde (PFA) in PBS. Brains were harvested, sliced into 6-mm coronal blocks in a brain matrix, post-fixed by immersion in 4% PFA/PBS overnight and then transferred to 30% (w/v) sucrose. Representative segments of the spinal cords at cervical, thoracic and lumbar levels were collected and post-fixed as well. A sliding microtome was used to cut serial 40-µm sections for histological processing.

To assess transgene expression, we performed immunohistochemistry with polyclonal antibodies against GFP (rabbit anti-GFP, 1:1000, G10362, www.lifetechnologies.com). Briefly, tissue sections were washed in PBS, blocked in 1% H_2O_2/30% alcohol/PBS, and then rinsed in PBST (PBS/1% Tween 20). Then incubated in Background Sniper blocking solution (Cat. BS966G; www.biocare.net) followed by a 24-h incubation at 4 °C with primary antibody against either GFP in Da Vinci Green diluent (PD900; www.biocare.net). The next day, sections were washed in PBST and incubated in Rabbit Mach 2 HRP-polymer (RP531L; www.biocare.net) at room temperature for 1 h. All sections were chromogenically developed with 3,3′-diaminobenzidine (DAB; DAB Peroxidase Substrate Kit, SK-4100, www.vectorlabs.com) according to the manufacturer's instructions. To study immune response, antibodies against glial fibrillary acidic protein (GFAP; mouse anti-GFAP, 1:100 000, MAB360 www.emdmillipore.com), ionized calcium-binding adaptor molecule 1 (Iba1; rabbit anti-Iba1, 1:1000, CP290C www.biocare.net), the major histocompatibility complex class II (MHC-II; mouse anti-MHC-II, 1:300, M3887-30, www.usbio.net) and neuronal protein NeuN (mouse anti-NeuN, 1:5000, MAB377, www.merckmillipore.com) were used separately with the immunoperoxidase staining protocol described above.

Standard hematoxylin and eosin (H&E) staining was performed on brain sections from all animals to detect pathological signs. Briefly, slide-mounted sections were washed in graded alcohol (100, 95 and 70% v/v; 3 min each), rehydrated in distilled water and stained in Gill II hematoxylin (www.leica-microsystems.com) for 3 min. After sections were washed, they were differentiated in 0.5% glacial acetic acid/70% alcohol, immersed in bluing solution and counterstained for 2 min in eosin Y (www.leica-microsystems.com). Finally, after washing them a final time, sections were dehydrated in alcohol (95 and 100%; 3 min each), immersed in fresh xylene (2×3 min), and coverslip and preserved with Shandon mounting medium (www.thermofisher.com).

Neutralizing activity analysis

Neutralizing antibodies against AAV5 capsid present in blood were analyzed before and after surgery. Typically, a cell-based

neutralizing antibody assay is used to determine the level of such antibodies, but, since the AAV serotype 5 does not transduce efficiently cells *in vitro*, an in-house enzyme-linked immunosorbent assay (ELISA) for total amount of IgG against AAV5 capsid was developed. It is well known that the titer of nAb against the capsid is proportional to the total amount of IgG against this capsid. Briefly, MaxiSorp 96-well plates (www.sigmaaldrich.com) were coated with AAV5-GFP vector at 3×10^{10} vg ml^{-1}. After blocking unspecific binding with Block & Sample Buffer (G3311; www.promega.com), serial dilutions of serum samples (from 1:50 to 1:6400) were added to the wells and incubated for 2 h at room temperature. After washing plates in Tris-buffered saline with Tween-20 (28360; www.thermofisher.com) goat anti-monkey IgG-HRP diluted with BS buffer at 1:20 000 (43R-IG020HRP; www.fitzgerald-fii.com) was added to all wells and the plates were incubated for 2 h. Following five washes in TBST buffer, samples were incubated for 5 min by adding SuperSignal ELISA Pico Chemiluminescent Substrate (37070; www.thermofisher.com) and then luminescence signal was detected by SpectraMax i3 plate reader (www.moleculardevices.com). The nAb production was measured by comparison to the signal from serum samples collected before the surgery. Fold differences were calculated by dividing normalized post-surgery and pre-surgery intensity values at 1:1600 dilution.

Study approval

All procedures were carried out with the approval of the Institutional Animal Care and Use Committee (IACUC), and in accordance with the Standard Operating Procedures protocol at Valley Biosystems, West Sacramento, CA, USA (IACUC permit: 14-10470).

CONFLICT OF INTEREST

Bas Blits and Harald Petry are employees and shareholders at UniQure. Krystof Bankiewicz and UCSF have a collaborative agreement with UniQure.

ACKNOWLEDGEMENTS

We thank Foad Green for his technical assistance in histology. UniQure funded the present study and provided the AAV5 viral vector for the experiments. We thank Jacek Lubelski for sharing his expertise on vector development.

REFERENCES

1 Bobo RH, Laske DW, Akbasak A, Morrison PF, Dedrick RL, Oldfield EH. Convection-enhanced delivery of macromolecules in the brain. *Proc Natl Acad Sci USA* 1994; **91**: 2076–2080.
2 Richardson RM, Kells AP, Rosenbluth KH, Salegio EA, Fiandaca MS, Larson PS *et al.* Interventional MRI-guided putaminal delivery of AAV2-GDNF for a planned clinical trial in Parkinson's disease. *Mol Ther* 2011; **19**: 1048–1057.
3 Richardson RM, Kells AP, Martin AJ, Larson PS, Starr PA, Piferi PG *et al.* Novel platform for MRI-guided convection-enhanced delivery of therapeutics: preclinical validation in nonhuman primate brain. *Stereotact Funct Neurosurg* 2011; **89**: 141–151.
4 Fiandaca MS, Forsayeth JR, Dickinson PJ, Bankiewicz KS. Image-guided convection-enhanced delivery platform in the treatment of neurological diseases. *Neurotherapeutics* 2008; **5**: 123–127.
5 Fiandaca MS, Varenika V, Eberling J, McKnight T, Bringas J, Pivirotto P *et al.* Real-time MR imaging of adeno-associated viral vector delivery to the primate brain. *NeuroImage* 2009; **47**: T27–T35.
6 Salegio EA, Samaranch L, Kells AP, Mittermeyer G, San Sebastian W, Zhou S *et al.* Axonal transport of adeno-associated viral vectors is serotype-dependent. *Gene Ther* 2013; **20**: 348–352.
7 Foust KD, Nurre E, Montgomery CL, Hernandez A, Chan CM, Kaspar BK. Intravascular AAV9 preferentially targets neonatal neurons and adult astrocytes. *Nat Biotechnol* 2009; **27**: 59–65.
8 Gray SJ, Matagne V, Bachaboina L, Yadav S, Ojeda SR, Samulski RJ. Preclinical differences of intravascular AAV9 delivery to neurons and glia: a comparative study of adult mice and nonhuman primates. *Mol Ther* 2011; **19**: 1058–1069.
9 Samaranch L, Salegio EA, San Sebastian W, Kells AP, Foust KD, Bringas JR *et al.* Adeno-associated virus serotype 9 transduction in the central nervous system of nonhuman primates. *Hum Gene Ther* 2012; **23**: 382–389.
10 Samaranch L, Salegio EA, San Sebastian W, Kells AP, Bringas JR, Forsayeth J *et al.* Strong cortical and spinal cord transduction after AAV7 and AAV9 delivery into the cerebrospinal fluid of nonhuman primates. *Hum Gene Ther* 2013; **24**: 526–532.
11 Ciesielska A, Hadaczek P, Mittermeyer G, Zhou S, Wright JF, Bankiewicz KS *et al.* Cerebral infusion of AAV9 vector-encoding non-self proteins can elicit cell-mediated immune responses. *Mol Ther* 2013; **21**: 158–166.
12 Samaranch L, San Sebastian W, Kells AP, Salegio EA, Heller G, Bringas JR *et al.* AAV9-mediated expression of a non-self protein in nonhuman primate central nervous system triggers widespread neuroinflammation driven by antigen-presenting cell transduction. *Mol Ther* 2014; **22**: 329–337.
13 Kells AP, Hadaczek P, Yin D, Bringas J, Varenika V, Forsayeth J *et al.* Efficient gene therapy-based method for the delivery of therapeutics to primate cortex. *Proc Natl Acad Sci USA* 2009; **106**: 2407–2411.
14 Kells AP, Forsayeth J, Bankiewicz KS. Glial-derived neurotrophic factor gene transfer for Parkinson's disease: anterograde distribution of AAV2 vectors in the primate brain. *Neurobiol Dis* 2012; **48**: 228–235.
15 Ciesielska A, Mittermeyer G, Hadaczek P, Kells AP, Forsayeth J, Bankiewicz KS. Anterograde axonal transport of AAV2-GDNF in rat basal ganglia. *Mol Ther* 2011; **19**: 922–927.
16 Thorne BA, Takeya RK, Peluso RW. Manufacturing recombinant adeno-associated viral vectors from producer cell clones. *Hum Gene Ther* 2009; **20**: 707–714.
17 Martin J, Frederick A, Luo Y, Jackson R, Joubert M, Sol B *et al.* Generation and characterization of adeno-associated virus producer cell lines for research and preclinical vector production. *Hum Gene Ther Methods* 2013; **24**: 253–269.
18 Hadaczek P, Stanek L, Ciesielska A, Sudhakar V, Samaranch L, Pivirotto P *et al.* Widespread AAV1- and AAV2-mediated transgene expression in the nonhuman primate brain: implications for Huntington's disease. *Mol Ther Methods Clin Dev* 2016; **3**: 16037.
19 Dong B, Duan X, Chow HY, Chen L, Lu H, Wu W *et al.* Proteomics analysis of co-purifying cellular proteins associated with rAAV vectors. *PLoS One* 2014; **9**: e86453.
20 San Sebastian W, Samaranch L, Heller G, Kells AP, Bringas J, Pivirotto P *et al.* Adeno-associated virus type 6 is retrogradely transported in the non-human primate brain. *Gene Ther* 2013; **20**: 1178–1183.
21 Green F, Samaranch L, Zhang HS, Manning-Bog A, Meyer K, Forsayeth J *et al.* Axonal transport of AAV9 in nonhuman primate brain. *Gene Ther* 2016; **23**: 520–526.
22 Matsuzaki Y, Konno A, Mukai R, Honda F, Hirato M, Yoshimoto Y *et al.* Transduction profile of the marmoset central nervous system using adeno-associated virus serotype 9 vectors. *Mol Neurobiol* 2016; doi:10.1007/s12035-016-9777-6.
23 Castle MJ, Perlson E, Holzbaur EL, Wolfe JH. Long-distance axonal transport of AAV9 is driven by dynein and kinesin-2 and is trafficked in a highly motile Rab7-positive compartment. *Mol Ther* 2014; **22**: 554–566.
24 Cressant A, Desmaris N, Vérot L, Bréjot T, Froissart R, Vanier M-T *et al.* Improved behavior and neuropathology in the mouse model of Sanfilippo type IIIB disease after adeno-associated virus-mediated gene transfer in the striatum. *J Neurosci* 2004; **24**: 10229–10239.
25 Ellinwood NM, Ausseil J, Desmaris N, Bigou S, Liu S, Jens JK *et al.* Safe, efficient, and reproducible gene therapy of the brain in the dog models of Sanfilippo and Hurler syndromes. *Mol Ther* 2011; **19**: 251–259.
26 Keiser MS, Boudreau RL, Davidson BL. Broad therapeutic benefit after RNAi expression vector delivery to deep cerebellar nuclei: implications for spinocerebellar ataxia type 1 therapy. *Mol Ther* 2013; **22**: 588–595.
27 Zabner J, Seiler M, Walters R, Kotin RM, Fulgeras W, Davidson BL *et al.* Adeno-associated virus type 5 (AAV5) but not AAV2 binds to the apical surfaces of airway epithelia and facilitates gene transfer. *J Virol* 2000; **74**: 3852–3858.
28 Rayaprolu V, Kruse S, Kant R, Venkatakrishnan B, Movahed N, Brooke D *et al.* Comparative analysis of adeno-associated virus capsid stability and dynamics. *J Virol* 2013; **87**: 13150–13160.
29 Emborg ME, Hurley SA, Joers V, Tromp DPM, Swanson CR, Ohshima-Hosoyama S *et al.* Titer and product affect the distribution of gene expression after intraputaminal convection-enhanced delivery. *Stereotact Funct Neurosurg* 2014; **92**: 182–194.
30 Davidson BL, Stein CS, Heth JA, Martins I, Kotin RM, Derksen TA *et al.* Recombinant adeno-associated virus type 2, 4, and 5 vectors: transduction of variant cell types and regions in the mammalian central nervous system. *Proc Natl Acad Sci* 2000; **97**: 3428–3432.
31 Nanou A, Higginbottom A, Valori CF, Wyles M, Ning K, Shaw P *et al.* Viral delivery of antioxidant genes as a therapeutic strategy in experimental models of amyotrophic lateral sclerosis. *Mol Ther* 2013; **21**: 1486–1496.

32 Merienne N, Douce JL, Faivre E, Déglon N, Bonvento G. Efficient gene delivery and selective transduction of astrocytes in the mammalian brain using viral vectors. *Front Cell Neurosci* 2013; **7**: 106.
33 Jakobsson J, Lundberg C. Lentiviral vectors for use in the central nervous system. *Mol Ther* 2006; **13**: 484–493.
34 Forsayeth J, Bankiewicz KS. Transduction of antigen-presenting cells in the brain by AAV9 warrants caution in preclinical studies. *Mol Ther* 2015; **23**: 612.
35 San Sebastian W, Kells AP, Bringas J, Samaranch L, Hadaczek P, Ciesielska A *et al.* Safety and tolerability of MRI-guided infusion of AAV2-hAADC into the mid-brain of non-human primates. *Mol Ther Methods Clin Dev* 2014; **3**. doi:10.1038/mtm.2014.49.
36 Urabe M, Ding C, Kotin RM. Insect cells as a factory to produce adeno-associated virus type 2 vectors. *Hum Gene Ther* 2002; **13**: 1935–1943.
37 Unzu C, Hervás-Stubbs S, Sampedro A, Mauleón I, Mancheño U, Alfaro C *et al.* Transient and intensive pharmacological immunosuppression fails to improve AAV-based liver gene transfer in non-human primates. *J Transl Med* 2012; **10**: 122.
38 Salegio EA, Bringas J, Bankiewicz KS. MRI-guided delivery of viral vectors. *Methods Mol Biol* 2016; **1382**: 217–230.
39 Bankiewicz KS, Eberling JL, Kohutnicka M, Jagust W, Pivirotto P, Bringas J *et al.* Convection-enhanced delivery of AAV vector in parkinsonian monkeys; in vivo detection of gene expression and restoration of dopaminergic function using pro-drug approach. *Exp Neurol* 2000; **164**: 2–14.
40 Krauze MT, Saito R, Noble C, Tamas M, Bringas J, Park JW *et al.* Reflux-free cannula for convection-enhanced high-speed delivery of therapeutic agents. *J Neurosurg* 2005; **103**: 923–929.

Supplementary Information accompanies this paper on Gene Therapy website (http://www.nature.com/gt)